

RESEARCH

Hotspot *DAXX*, *PTCH2* and *CYFIP2* mutations in pancreatic neuroendocrine neoplasms

T Vandamme^{1,2,*}, M Beyens^{1,*}, G Boons¹, A Schepers³, K Kamp², K Biermann⁴, P Pauwels⁵, W W De Herder², L J Hofland², M Peeters¹, G Van Camp³ and K Op de Beek¹

¹Center of Oncological Research (CORE), University of Antwerp, Antwerp, Belgium

²Section of Endocrinology, Department of Internal Medicine, Section of Endocrinology, Erasmus Medical Center, Rotterdam, The Netherlands

³Center of Medical Genetics, University of Antwerp, Antwerp, Belgium

⁴Department of Pathology, Erasmus Medical Center, Rotterdam, The Netherlands

⁵Department of Pathology, University of Antwerp, Antwerp, Belgium

Correspondence should be addressed to T Vandamme: timon.vandamme@uantwerpen.be

*(T Vandamme and M Beyens contributed equally to this work)

Abstract

Mutations in *DAXX/ATRX*, *MEN1* and genes involved in the phosphoinositide-3-kinase/Akt/mammalian target of rapamycin (PI3K/Akt/mTOR) pathway have been implicated in pancreatic neuroendocrine neoplasms (pNENs). However, mainly mutations present in the majority of tumor cells have been identified, while proliferation-driving mutations could be present only in small fractions of the tumor. This study aims to identify high- and low-abundance mutations in pNENs using ultra-deep targeted resequencing. Formalin-fixed paraffin-embedded matched tumor-normal tissue of 38 well-differentiated pNENs was sequenced using a HaloPlex targeted resequencing panel. Novel amplicon-based algorithms were used to identify both single nucleotide variants (SNVs) and insertion-deletions (indels) present in >10% of reads (high abundance) and in <10% of reads (low abundance). Found variants were validated by Sanger sequencing. Sequencing resulted in 416,711,794 reads with an average target base coverage of 2663 ± 1476 . Across all samples, 32 high-abundance somatic, 3 germline and 30 low-abundance mutations were withheld after filtering and validation. Overall, 92% of high-abundance and 84% of low-abundance mutations were predicted to be protein damaging. Frequently, mutated genes were *MEN1*, *DAXX*, *ATRX*, *TSC2*, PI3K/Akt/mTOR and MAPK-ERK pathway-related genes. Additionally, recurrent alterations on the same genomic position, so-called hotspot mutations, were found in *DAXX*, *PTCH2* and *CYFIP2*. This first ultra-deep sequencing study highlighted genetic intra-tumor heterogeneity in pNEN, by the presence of low-abundance mutations. The importance of the *ATRX/DAXX* pathway was confirmed by the first-ever pNEN-specific protein-damaging hotspot mutation in *DAXX*. In this study, both novel genes, including the pro-apoptotic *CYFIP2* gene and hedgehog signaling *PTCH2*, and novel pathways, such as the MAPK-ERK pathway, were implicated in pNEN.

Key Words

- ▶ neuroendocrine tumors
- ▶ molecular genetics
- ▶ ultra-deep sequencing
- ▶ pancreatic neuroendocrine tumors
- ▶ DAXX

Endocrine-Related Cancer
(2019) **26**, 1–12

Introduction

Neuroendocrine neoplasms of the pancreas (pNENs), originating from the islet cells, are considered rare, although incidence is increasing (Dasari *et al.* 2017). pNENs can occur as part of genetic syndromes, such as multiple neuroendocrine neoplasia 1 (MEN1), Von-Hippel Lindau and tuberous sclerosis complex. However, most pNENs are sporadic tumors without familial history of NENs (Crona & Skogseid 2016). Recently, non-familial pNENs have been genetically characterized using whole-exome and whole-genome sequencing in large cohorts of 40–102 patients (Jiao *et al.* 2011, Sadanandam *et al.* 2015, Scarpa *et al.* 2017). These studies identified *MEN1* as most frequently mutated gene, in frequencies ranging from 37 to 44% of all sequenced tumors. Additionally, *DAXX* was found to be mutated in 22–25% of all tumor samples, while *ATRX* was mutated in 10–17% of all tumors. Menin (the *MEN1* protein), *DAXX* and *ATRX* are epigenetic regulators. Menin is involved in histone modification, while *ATRX* and *DAXX* play a role in alternative telomere lengthening and chromatin remodeling (Elsasser *et al.* 2011, Heaphy *et al.* 2011). Additionally, mutations in genes involved in the phosphoinositide-3-kinase/Akt/mammalian target of rapamycin (PI3K/Akt/mTOR) pathway were found in 12–14% of tumors (Jiao *et al.* 2011, Scarpa *et al.* 2017). In the pivotal Radiant-3 trial, treatment with everolimus, an mTOR inhibitor, has demonstrated an improved progression-free survival in advanced pNENs (Yao *et al.* 2011). Hence, alterations in the PI3K/Akt/mTOR pathway, such as mutations in *PTEN*, could have clinical implications. However, no molecular predictive biomarker for everolimus treatment has yet been identified. Frequent tumor-specific copy number alterations in *MEN1*, *ATRX*, *DAXX* and PI3K/Akt/mTOR genes implicate these core pathways further (Scarpa *et al.* 2017). Recent efforts to describe molecular subtypes have led to the identification of five mutational signatures in pNEN, including the novel *MUTYH* signature (Scarpa *et al.* 2017). However, in more than 50% of all tumors, no dominant mutational signature could be identified (Scarpa *et al.* 2017). RNA expression analysis revealed three expression subtypes, respectively the insulinoma, MEN-1-like/intermediate and metastasis-like (MLP) subtype (Sadanandam *et al.* 2015, Scarpa *et al.* 2017). Clinical utility of these expression subtypes is subject of further study, as expression subtypes show a variable association with tumor grade, mainly in WHO 2010 grade 1 and 2 tumors (Sadanandam *et al.* 2015). Moreover, within-patient and within-tumor heterogeneity in proliferation

has been demonstrated in neuroendocrine neoplasm models and patients (Shi *et al.* 2015, Vandamme *et al.* 2015a, 2016). In recent pNEN sequencing studies, average sequencing depth was 61- to 102-fold (Sadanandam *et al.* 2015, Scarpa *et al.* 2017). Although covering all the genome, these studies might lack sequencing power to reliably detect mutations present in a fraction of the cells, as these rare alleles might be present in less than 1 in 100 sequencing reads on a given genomic position (Gerstung *et al.* 2012). Therefore, current studies lack information on mutational heterogeneity. By increasing sequencing depth, mutations, present in a fraction of cells, can be reliably identified (Gerstung *et al.* 2012). This study is the first to use an ultra-deep targeted resequencing approach in pNENs to elucidate mutations, present in less than 10% of sequencing reads.

Materials and methods

Sample collection and clinical data

Patients diagnosed between 1997 and 2013 with a reported WHO 2010 grade 1 or 2 pNEN were retrospectively included in this study (Bosman *et al.* 2010). Patients with a familial syndrome were excluded. Formalin-fixed paraffin-embedded (FFPE) samples of tumor and matched distant normal tissue, if available, of all patients was collected at the Erasmus Medical Center (Rotterdam, the Netherlands) and the Antwerp University Hospital (Antwerp, Belgium). All samples were reviewed by a dedicated pathologist for histology, Ki67 index, mitoses per high power field and tumor purity. Only samples with estimated tumor purity >60% on hematoxylin and eosin-stained histological slide, after macrodissection, were included. Data on age, sex, TNM stage, age at diagnosis, secretion status, received treatments, disease-free survival and overall survival were collected. The study was approved by the Institutional Human Ethics Review Board of the Antwerp University Hospital. Informed consent was obtained from all patients for the use of excess tissue material for scientific research, based on the opt-out registry to document the objection of patients (as specified in Belgian and Dutch law).

Targeted gene panel development

A custom HaloPlex enrichment panel (Agilent Technologies) was developed to sequence all exons of 20 genes (Table 1). Genes were selected based upon patient and cell line sequencing results (Jiao *et al.* 2011, Vandamme *et al.* 2015b). PI3K/Akt/mTOR pathway-related

Table 1 List of genes (including encoded protein, chromosomal positions and number of exons) and the calculated coverage of the custom HaloPlex enrichment panel.

RefSeq gene id	Encoded protein	Chromosomal position	Exons	Size (bp)	Coverage (%)
PI3K/AKT/mTOR pathway					
<i>MTOR</i>	Mechanistic target of rapamycin	chr1:11166651-11319476	60	9217	99.75
<i>PIK3C2A</i>	Phosphatidylinositol-4-phosphate 3-kinase catalytic subunit type 2 alpha	chr11:17111274-17191298	32	5705	100
<i>PIK3CA</i>	Phosphatidylinositol-4,5-bisphosphate 3-kinase catalytic subunit alpha	chr3:178916603-178952162	20	3609	99.5
<i>PTEN</i>	Phosphatase and tensin homolog	chr10:89624216-89725239	9	1392	100
<i>TSC2</i>	Tuberous sclerosis 2	chr16:2098260-2138621	43	6592	98.07
Transcription/chromatin remodeling					
<i>ATRX</i>	ATRX, chromatin remodeler	chrX:76763818-77041497	37	8299	99.92
<i>DAXX^a</i>	Death domain associated protein	chr6:33286509-33290701	8	2436	100
<i>KANSL1</i>	KAT8 regulatory NSL complex subunit 1	chr17:44108831-44249519	14	3598	100
<i>MEN1</i>	Menin 1	chr11:64571795-64577591	9	2028	100
<i>PIF1</i>	PIF1 5'-to-3' DNA helicase	chr15:65107879-65116544	13	2444	100
MAPK/ERK pathway					
<i>KRAS</i>	KRAS proto-oncogene, GTPase	chr12:25362718-25398328	6	828	100
<i>MAP4K2</i>	Mitogen-activated protein kinase kinase kinase 2	chr11:64556998-64570631	32	3103	100
<i>MAPK9</i>	Mitogen-activated protein kinase 9	chr5:179663373-179707571	14	1943	100
<i>MAPKBP1</i>	Mitogen-activated protein kinase binding protein 1	chr15:42067463-42117644	32	5461	100
p53 pathway					
<i>CYFIP2</i>	Cytoplasmic FMR1 Interacting Protein 2	chr5:156712361-156820018	34	4543	99.89
<i>TP53</i>	Tumor protein p53	chr17:7565246-7579922	14	1697	97.88
G protein-coupled receptor (GPCR) signaling pathway					
<i>KISS1</i>	KISS-1 metastasis-suppressor	chr1:204159601-204162014	2	457	100
Hedgehog signaling pathway					
<i>PTCH2</i>	Patched 2	chr1:45286350-45308614	24	4171	100
TGF- β signaling pathway					
<i>SMAD4</i>	SMAD family member 4	chr18:48573406-48604847	13	1999	100
Wnt signaling pathway					
<i>WNT1</i>	Wnt family member 1	chr12:49372423-49375433	4	1193	100

^aMultifunctional protein also associated with FAS signaling pathway.

genes *MTOR*, *PTEN*, *PIK3CA* and *TSC2* mutations have been found in pNEN patients and could have therapeutic implications (Jiao *et al.* 2011, Grabiner *et al.* 2014, Scarpa *et al.* 2017). The gene panel was extended with the PI3K-related *PIK3C2A* gene, as it was found mutated in pNEN cell line data (Vandamme *et al.* 2015b). Epigenetic modifiers could play a role in pNEN, as demonstrated by *MEN1*, *ATRX* and *DAXX* mutations identified previously in pNEN (Jiao *et al.* 2011, Scarpa *et al.* 2017). Next to these genes, *KANSL1* and *PIF1*, two epigenetic modifiers found in pNEN cell line data, were included in the panel (Vandamme *et al.* 2015b). As preclinical data suggests a role for the MAPK/ERK pathway in pNEN, *KRAS*, *MAP4K2*, *MAPK9* and *MAPKBP1* were added to the panel (Valentino *et al.* 2014, Vandamme *et al.* 2016). The *SMAD4* gene has been found mutated in neuroendocrine neoplasms, both in patient material and in cell lines (Bartsch *et al.* 1999, Vandamme *et al.* 2015b). *TP53* and *CYFIP2* are two genes involved in apoptosis that are frequently implicated in oncogenesis. Both genes were found mutated in pNEN cell line data and were hence added to the panel (Vandamme *et al.* 2015b). Finally, the panel was extended with three genes (*KISS1*, *PTCH2*, *WNT1*) in known cancer-related pathways. All genes contained mutations in pNEN cell line data (Vandamme *et al.* 2015b). In our custom HaloPlex primer design, 99.59% of the 70,715 target kilobases of selected genes were covered by developed primers. The primer design was optimized for use with FFPE material and for sequencing on Illumina technology with a read length of 150 base pairs by increasing the number of amplicons to 19,838.

DNA isolation, HaloPlex enrichment and sequencing

After macrodissection, ten slides of 5 µm of both tumor and normal tissue were used as input for DNA isolation using the QIAamp DNA FFPE Tissue Kit (Qiagen), following manufacturer's instructions. The concentration of the isolated DNA was quantified using the Qubit 2.0 fluorometer with the dsDNA Broad Range Assay (Thermo Scientific). To determine the amount of input DNA for HaloPlex enrichment, quality and degradation of the DNA were checked following the FFPE-Derived DNA Quality Assessment-protocol (Agilent Technologies) using the LabChip GX (PerkinElmer) with a High-Sensitivity DNA kit (PerkinElmer). Next, all tumor samples and three representative normal samples were prepared for targeted resequencing using a custom HaloPlex Design enrichment, optimized for FFPE sample enrichment, following the FFPE-optimized protocol according to

manufacturer's instructions. The enriched samples were hybridized, amplified and sequenced on two lanes of a paired-end flow cell using HiSeq 1500 (Illumina, San Diego, USA) platform in rapid run mode.

Read alignment, variant calling and filtering

Raw sequencing reads were analyzed using an in-house developed Perl-based workflow. First, FastQC software (version 1.0) was used to assess quality of the raw data (Andrews 2010). Adapters and low-quality bases were trimmed using Cutadapt (version 1.2.1) and an in-house developed paired-end read quality trimmer (Vandeweyer *et al.* 2014), respectively. Paired-end reads were then aligned to the human reference genome (hg19, NCBI Build 37) using Burrows-Wheeler Aligner (BWA mem, version 0.7.3a) (Li & Durbin 2009). Picard (version 1.88) was used to mark and remove duplicates. Afterward, the three aligned normals were merged using Samtools (version 0.1.18) (Li *et al.* 2009). After merging, somatic variant calling was performed on the tumor aligned data with VarScan2 (version 2.3.9) using the three merged normals as one merged normal (Koboldt *et al.* 2012). Alignments with mapping quality lower than 17 or nucleotides with base quality lower than 17 were ignored. The max per-BAM depth was set on 30,000 avoiding excessive memory usage. No correction for tumor purity was set during the somatic calling, purities were kept on default (100%). The variant calling files were first filtered using pyAmpli to eliminate false-positive variants introduced by amplicon-based enrichment (Beyens *et al.* 2017). All variants were annotated with ANNOVAR (Wang *et al.* 2010), and filtered using VariantDB (Vandeweyer *et al.* 2014) according to different criteria (Results section). Identified variants were validated in tumor and its matching normal tissue, if available, with Sanger sequencing on the 3130xl Genetic Analyzer (Applied Biosystems Inc.) platform and analyzed using CLC DNA Workbench v5 software (CLC Bio, Aarhus, Denmark). Data were visualized using the Maftools package (Mayakonda & Koeffler 2016) in R (version 3.3.3). Survival statistics were generated using the survival and survminer package for R (version 3.3.3).

Results

Patient characteristics

Thirty-eight pNEN patients were included, of which 51% were male. Of the 38 included patients, 13 patients had a functional tumor (11 insulinomas, one gastrinoma

and one glucagonoma). Mean age at diagnosis was 53 ± 14 years. Of all patients, 9 (16%) had metastatic disease at diagnosis (Supplementary Table S1, see section on [supplementary data](#) given at the end of this article). Tumor tissue was available for all included patients, while matched normal tissue was collected in 27 patients (71%). Twenty-four patients were diagnosed with WHO grade 1 disease, while 13 patients had a WHO grade 2 tumor. Upon central pathology review, one patient was reclassified as a WHO 2010 grade 3 tumor, given the Ki67 index of 30%. Median follow-up time was 6.3 years (range: 1.9–19.2 years). Median overall survival was 13 years (95% CI 11 years – not reached).

Genetic alterations in pNENs

Targeted resequencing of the selected HaloPlex enrichment 20-gene panel (see Materials and methods) resulted in a total of 416,711,794 reads, passing quality filtering, across 38 tumor samples and three normal samples. Of all reads, an average $80.4 \pm 5.0\%$ mapped on target regions. Average target base coverage was 2663 ± 1476 and $94.7 \pm 1.9\%$ of all target bases was covered at least 30 times. Using VarScan2, variants in the tumor were called against three merged normal samples. Afterward, the amplicon-based filtering method pyAmpli was deployed to withhold only alterations present in more than one amplicon (if more than one amplicon was in the enrichment design) (Beyens *et al.* 2017). Additionally, all variants that were marked as ‘somatic’ by VarScan2 were withheld. By this combined elimination, genetic alterations that are inherent to the enrichment with the HaloPlex panel and, hence, appear in all amplicons across all samples, are removed as false positive. Additionally, genetic alterations that are present in all three sequenced normal samples will most likely not be oncogenic driver mutations. Hence, these mutations can be discarded as common polymorphisms or artifacts when they are seen in the tumor samples. After this combined filtering, 17 indels and 2270 single nucleotide variations (SNVs) were withheld in the 38 tumors. The resulting median mutation burden of 0.80 per Megabase (Mb, range 0.51–1.54) within the 20 selected genes, with a genomic length of 70.71 Mb, is in line with the previously reported genome-wide mutation burden of 0.82 per Mb in pNEN and is low in comparison to other tumor types (Scarpa *et al.* 2017). Although caution is needed when comparing mutation burden between the targeted sequencing panel and the previously reported whole-genome data, it seems that the 20 selected genes in the targeted panel show no enrichment for mutations

in comparison to other genomic regions. Before further filtering, the median number of genetic alterations per tumor was 56 with the *MTOR* gene containing the most alterations (Fig. 1). The most frequent nucleotide substitutions were C \leftrightarrow T transitions (Fig. 1). Across all samples, transitions made up $63.4 \pm 2.3\%$ of the filtered SNVs, resulting in a ratio of transitions to transversions of 1.74 ± 0.18 in the presented gene panel. In human germline samples, an average transitions to transversion rate of 1.7 is usually seen genome-wide (Lynch 2010). A genome-wide mutation spectrum with a predominant C to T/G to A transition pattern is seen in many adult cancers, including melanoma, breast, lung, colorectal, ovarian and pancreas adenocarcinoma (Greenman *et al.* 2007, Jones *et al.* 2008). However, in pNENs, a more even distribution of transversions and transitions has been reported previously, in line with the data in this study (Jiao *et al.* 2011).

Identification and validation of somatic and germline mutations

To identify mutations with possible functional impact, RefSeq synonymous as well as intronic SNVs and intronic indels were first removed from further analysis (Pruitt *et al.* 2014). To eliminate common SNPs, only variants with a minor allele frequency (MAF) smaller than 0.05 in the dbSNP v142, ESP65000 and 1000 Genomes databases were withheld (Sherry *et al.* 2001, Genomes Project *et al.* 2010). Final visual inspection of all remaining variants in Integrative Genomics Viewer (IGV version 2.2.5), led to the identification of 72 mutations with possible functional impact (Fig. 2) (Thorvaldsdottir *et al.* 2012). Of these 72 mutations, 42 alterations were identified in more than 10% of sequencing reads at that genomic position and were considered high-abundance alterations. These 42 alterations were Sanger sequenced in tumor tissue. Additionally, of 27 patients (71%) corresponding normal tissue was available, allowing Sanger sequencing of normal tissue for 22 mutations. Out of the 42 high-abundant variants, 35 were validated through Sanger sequencing, while 6 variants could not be detected in the Sanger electropherogram traces. For one variant, PCR amplification of the tumor DNA region containing the variant was unsuccessful, despite successful amplification in control DNA and use of different primers. Overall, 83.3% of all high-abundant variants could be validated (Supplementary Table S2). The 35 validated mutations contained three germline RefSeq non-synonymous variants, one in *MAPKBP1* and two in *PIF1* respectively,

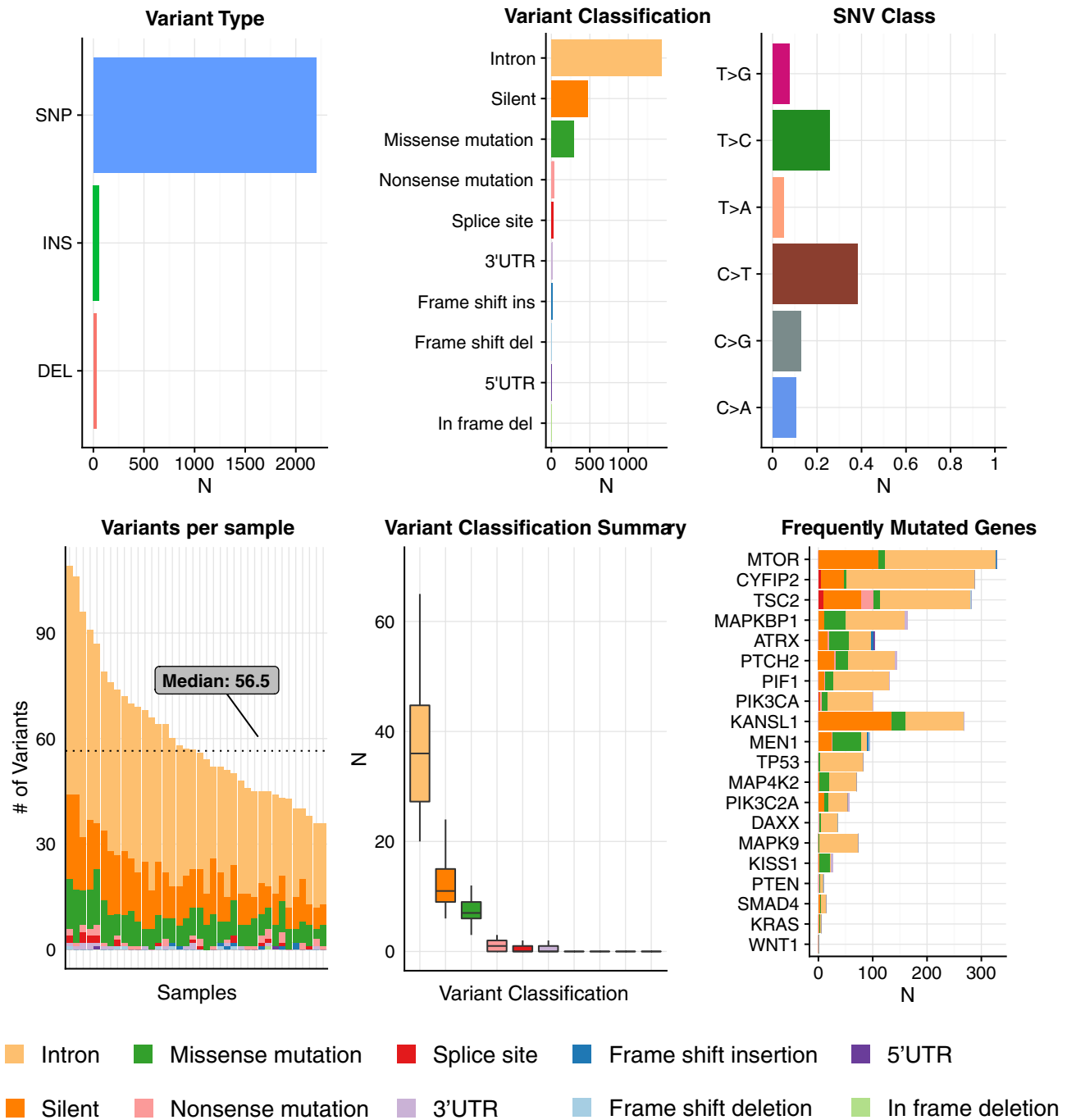
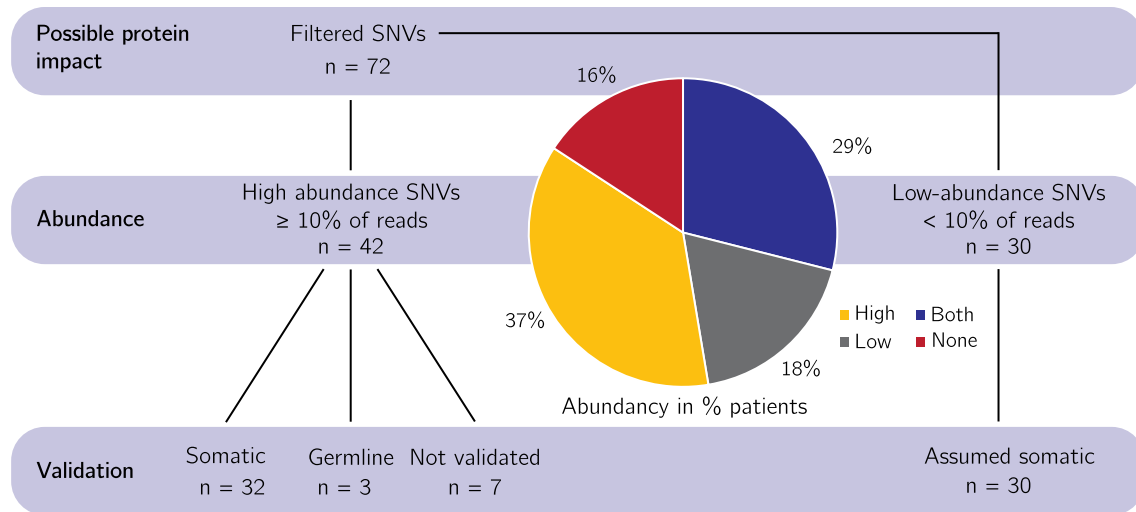


Figure 1 Summary plot of SNVs ($N = 2270$), insertions ($N = 9$) and deletions ($N = 8$) of all 38 samples, after amplicon-based filtering.

all unique in three different tumors. None of the mutations were present in the cancer somatic mutation COSMIC v70 database (accession date: 12th April 2017), while two SNVs were reported in the dbSNP142 database with unknown clinical significance, respectively dbSNP142 rs139868280 (*PIF1*) and rs201725344 (*MAPKBP1*) (Sherry *et al.* 2001,

Forbes *et al.* 2017). The other *PIF1* chr15:g.65108822C>T mutation was not found in any of the queried databases, including ExAc (version 03), 1000 Genomes Project (October 2014), dbSNP142 and COSMIC v70 (Sherry *et al.* 2001, Genomes Project *et al.* 2010, Lek *et al.* 2016, Forbes *et al.* 2017).

**Figure 2**

Filter strategy and abundance of mutations across tumors. Filtered variants are SNVs or indels that are not RefSeq synonymous or intronic and have a minor allele frequency (MAF) ≤ 0.05 in dbSNP v142, ESP65000 and 1000 Genomes. Abundance is considered low for alterations found in $< 10\%$ of targeted resequencing reads in tumor tissue and high when an alteration is present in $\geq 10\%$ of targeted resequencing reads. Mutation are validated somatic when mutation is present in Sanger sequencing of tumor but not in normal (if available). Germline mutations are present in Sanger sequencing traces of both tumor and normal tissue. Not validated SNVs are those SNVs with absent Sanger traces or inconclusive results. All low-abundance SNVs or indels are assumed to be somatic. Pie-chart shows the percentage of patients whose tumors contained only low-abundance mutations (gray), only high-abundance mutations (yellow), both (red) or no mutations (blue).

Abundant mutations include a DAXX and CYFIP2 hotspot mutation

Of the 32 validated high-abundant somatic mutations, 21 SNVs were annotated as non-synonymous by RefSeq, six as frameshift indels, three as stopgain SNVs, one as SNV in the 3'-UTR and one as nonframeshift indel. The most commonly mutated gene was *DAXX* with five high-abundance mutations, while four high-abundance mutations were found in *MEN1*, *MAP4K2* and *PTCH2*. *ATRX*, *KANSL1*, *TSC2* and *MAPKB1* each contained three high-abundance mutations. These 8 genes accounted for 80% of all validated high-abundance mutations. No high-abundance mutations were found in *PIF1*, *PIK3CA*, *PTEN*, *MAPK9*, *KRAS* and *TP53*. Using variantDB, all variants were annotated for functional impact prediction using the MutationAssessor, MutationTaster, Provean and PolyPhen algorithms (Vandeweyer *et al.* 2014). Of all variants, 92.0% was predicted damaging by at least one algorithm, while 36.0% was predicted damaging by at least three algorithms. Three mutations were also seen in other tumor types, according to the COSMIC database (Forbes *et al.* 2017). Two recurrent, so-called hotspot, mutations were found, one in *CYFIP2* and one in *DAXX*. The *CYFIP2* non-synonymous variant g.156766140G>A (NM_001037333, p.D820N) was found in two pNEN tumors. This variant had previously been identified in skin squamous cell carcinoma, according to COSMIC,

and was predicted to be damaging by MutationTaster and PROVEAN (Choi *et al.* 2012, Schwarz *et al.* 2014). Within the *DAXX* gene, one genomic position was altered differently in two tumors, yielding the non-synonymous g.33289247G>A (NM_001141970.1, p.S102L) and the stopgain g.33289247G>T (NM_001141970.1, p.S102X) mutations. Both mutations were predicted to be damaging by all used prediction algorithms, pointing toward a very likely *DAXX* loss-of-function in these tumors. The non-synonymous g.33289247G>A *DAXX* mutations has previously been found as a somatic mutation in one lung squamous cell carcinoma, according to COSMIC.

Low-abundance mutations contain a hotspot mutation in PTCH2

Next to high-abundance mutations, 30 mutations were found in less than 10% of targeted resequencing reads in tumor tissue. These mutations are considered low-abundance mutations. As the detection limit of Sanger sequencing is around 10%, these low-abundant alterations could not be Sanger sequenced (Tsiatis *et al.* 2010). However, the Sanger sequencing validation rate of 83% in the high-abundant mutations demonstrates that the used combined filtering strategy (see above) yields mainly true positives. Additionally, only 9% of validated mutations was present in corresponding

normal samples, illustrating that the employed filtering strategy selects for somatic variants. Hence, we assume that most of the low-abundance mutations are also both valid and somatic. RefSeq annotated 21 of these 30 low-abundance mutations as non-synonymous SNVs, four as frameshift indels, three as stopgain SNVs, one as splicing SNV and one as SNV in the 3'-UTR. The 3'-UTR *PIK3C2A* g.17111197_17111198del was found in three tumors. In addition, two intronic variants were found, the *DAXX* g.33286734A>C which was seen in 8 pNENs, and the *TSC2* g.2124481_2124482insG, identified in five tumors. However, functional impact of these intronic mutations remains unclear. When predicting protein impact on the 26 exonic SNVs with the MutationAssessor, MutationTaster, Provean and PolyPhen algorithms using variantDB, 84.0% of all SNVs was predicted damaging by at least one algorithm, while 52.0% was predicted to be damaging by three or more prediction algorithms (Vandeweyer *et al.* 2014). After inclusion of the four frameshift indels, which can be considered to have a deleterious impact on protein function, 86.6% of all mutations have a likely protein impact. Three mutations were previously found in cancer samples, according to the COSMIC database, including the non-synonymous *TP53* g.7578457C>T mutation (NM_001276695.1, p.R158H), which was identified in 36 tumors of various origin (Forbes *et al.* 2017). Two tumors

contained the same stopgain g.45292871C>A mutation (NM_001166292, p.G828X) in *PTCH2*, predicted to be damaging by MutationTaster, PROVEAN and SIFT. This protein-damaging *PTCH2* mutation is hence a novel low-abundance hotspot mutation within pNEN.

Mutational signatures in pNEN

In total, 32 tumors contained mutations while 6 tumors had no mutations that survived filtering (Fig. 3). Both low-abundance and high-abundance mutations were seen in 11 tumors (29%). High-abundance mutations were seen exclusively in 14 tumors (37%), while 7 tumors (18%) only contained low-abundance mutations (Fig. 2). *MEN1* was mutated most frequently in 8 out of 38 tumors (21%). *DAXX* and *ATRX* were both mutated in 5 out of 38 tumors (13%). The PI3K/Akt/mTOR-related gene *TSC2* was mutated in 7 out of 38 tumors (18%). Overall, mutations in PI3K/Akt/mTOR-related genes were seen in 29% of the tumors, including a validated non-synonymous g.1308007C>T mutation in *MTOR* (NM_004958, p.A329T, rs35903812) not previously reported in pNEN. The mitogen-activated kinase and extracellular signal-regulated kinase (MAPK-ERK pathway) genes *MAP4K2* and *MAPKBP1* were each mutated in three tumors.

Gene mutation plot after filtering

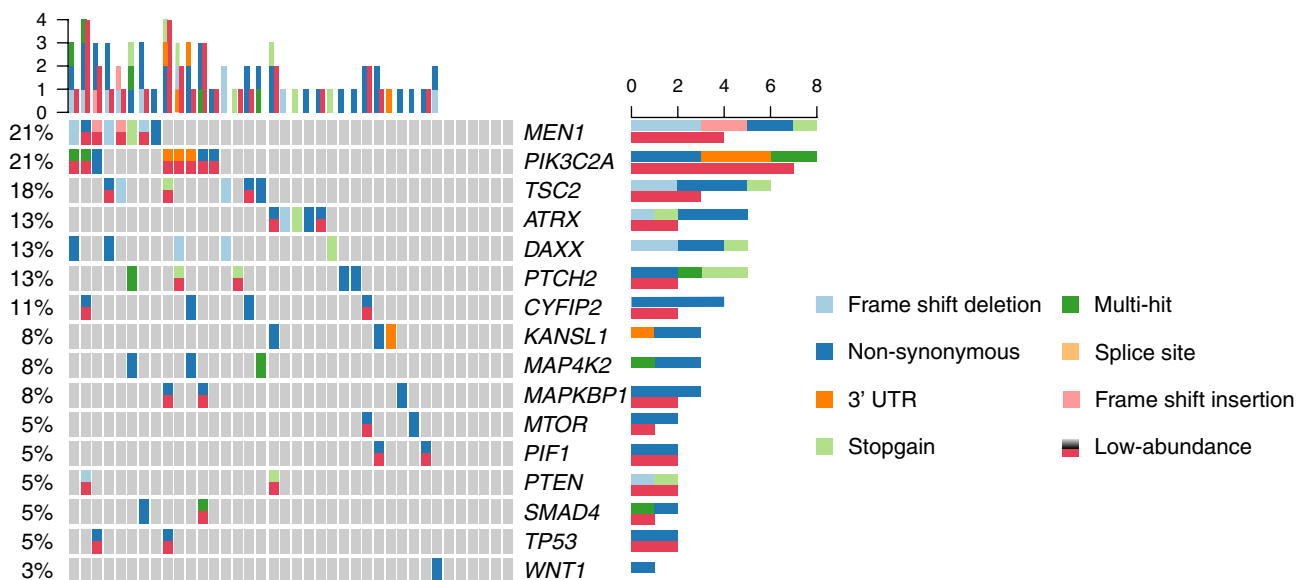


Figure 3

Mutation plot showing frequency, type of mutations, abundance and mutational distribution of genetic alterations across 38 included tumors, after filtering and validation (if executed), including both high-abundance ($N = 32$) and low-abundance ($N = 30$) mutations. Low-abundance mutations are marked with red, in addition to color-coded mutation type. When a tumor contains multiple mutations within one gene, this is annotated as multi-hit (dark green).

Discussion

This study presents the first ultra-deep targeted resequencing of pNENs in archival tissue. The relative rarity of pNENs has led to only a limited number of large-scale studies on the genetic constitution of pNENs (Jiao *et al.* 2011, Sadanandam *et al.* 2015, Scarpa *et al.* 2017). Additionally, these studies focus on a broad overview of frequent genetic alterations in pNEN and report high-abundance mutations. These high-abundance mutations are present in the majority of tumors cells. However, various studies have demonstrated that the genetic make-up of primary tumors evolves dynamically in time (Stratton *et al.* 2009, Burrell *et al.* 2013). This time-dependent change of the genetic alterations present in a tumor reflects the appearance and disappearance of subsets of tumor cells, so-called subclones, within one tumor (Stratton *et al.* 2009, Burrell *et al.* 2013). In our study, the use of ultra-deep sequencing allowed for the identification of genetic alterations that are present in a low fraction of the tumoral tissue, so-called low-abundance mutations. These low-abundance mutations are indicative for the genetic heterogeneity within a single tumor. Recent genetic studies have identified the insulinoma, MEN-1-like/intermediate and metastasis-like (MLP) RNA expression subtype in pNENs (Sadanandam *et al.* 2015). Although the MEN-1-like tumors frequently contains *MEN1* mutations, the mutational burden of high-abundance mutations in other core pathways seems to be more variable across subtypes (Sadanandam *et al.* 2015). Additionally, DNA damage repair, chromatin modification, alternated telomere length and the PI3K/Akt/mTOR pathways have been highlighted as core altered pathways in pNEN (Jiao *et al.* 2011, Scarpa *et al.* 2017). In this study, we demonstrate that low-abundance mutations are found in these pathways. Hence, low-abundance mutations might help to better classify tumors. However, validation of these low-abundance mutations remains complex and its lack forms a limitation of our study. The gene with the most high-abundance mutations within our study was the tumor suppressor gene *DAXX*. *ATRX* and *DAXX* form a complex facilitating the incorporation of histone variant H3.3 at the telomeres and, consequently, play a role in alternative lengthening of telomeres (Lewis *et al.* 2010, Heaphy *et al.* 2011). In many cancer types, it has been demonstrated that alternative telomere lengthening (ATL) leads to a prolonged cell survival, which is a hallmark of cancer (Cesare & Reddel 2010). In pNEN, ATL has been associated with a reduced disease-free survival (Singhi *et al.* 2017). Additionally, loss of *ATRX* and *DAXX* on

immunohistochemistry (IHC) staining, caused by inactivating mutations or copy number loss is associated with increased occurrence of metastasis and reduced disease-free survival (Scarpa *et al.* 2017, Singhi *et al.* 2017). Both high- and low-abundance mutations in *DAXX* and *ATRX* were identified in this study, including the first-ever validated recurrent, hotspot, mutation in *DAXX*, with likely loss-of-function on protein level. In line with other studies, exonic (transcript coding or protein encoding) mutations in *DAXX* and *ATRX* were mutually exclusive (Jiao *et al.* 2011, Scarpa *et al.* 2017). As this is the first study to demonstrate the existence of low-abundance mutations in *ATRX* and *DAXX*, conclusions on clinical impact are limited. Nonetheless, detection of low-abundance mutations might lead to the identification of *DAXX* and *ATRX* loss before this is apparent on IHC and, thus, an earlier identification of high-risk patients. Given the low number of events in the studied population (both in disease-recurrence and in mortality), this study is not adequately powered to evaluate prognostic relevance of these low-abundance mutations. Hence, further studies are needed. Menin, the nuclear protein encoded by *MEN1*, impacts ATL by negatively regulating hTERT (Lin & Elledge 2003). Additionally, it plays a key role in chromatin remodeling and gene expression through histone acetylation and deacetylation (Kim *et al.* 2003). *MEN1* mutations have been implicated in pNEN oncogenesis, both as part of the familial *MEN1* syndrome, and in sporadic tumors (Corbo *et al.* 2010, Jiao *et al.* 2011, Crona & Skogseid 2016, Scarpa *et al.* 2017). In 12–14% of all pNEN patients, a mutation in PI3K/Akt/mTOR-related genes is reported, including mutations in *PTEN*, *MTOR*, *DEPDC5*, *TSC1*, *TSC2* and *PIK3CA* (Jiao *et al.* 2011, Chou *et al.* 2016, Scarpa *et al.* 2017). In this study, PI3K/Akt/mTOR-related mutations could be identified in 29% of all tumors, including a novel p.A329T mutation in *MTOR* in pNEN. This increased frequency of mutations in the PI3K/Akt/mTOR-related genes is due to the detection of low-abundance mutations in these tumor samples. The relation of everolimus efficacy and PI3K/Akt/mTOR pathway-related mutations remains the subject of study in pNEN. However, in other cancer types, mutations of the PI3K/Akt/mTOR pathways seem to confer everolimus sensitivity (Grabiner *et al.* 2014, Wagle *et al.* 2014). In neuroendocrine neoplasms and other cancer types, cross-talk activation between the PI3K/Akt/mTOR pathway and the mitogen-activated kinase and extracellular signal-regulated kinase (MAPK-ERK pathway) through PI3K has been described (Carracedo *et al.* 2008, Zitzmann *et al.* 2010, Valentino *et al.* 2014). Until now, no mutations

in MAPK-ERK pathway-related genes have been reported in pNEN. In this study, mutations in *MAP4K2* and *MAPKBP1* were identified, further implicating this pathway in pNEN and providing additional rationale for the use of MEK-inhibitors in pNEN, either in combination with mTOR inhibitors or alone. Although *TP53* is frequently mutated in other cancers, *TP53* mutation frequency is low in pNEN, as demonstrated by only two low-abundance *TP53* mutations being present in our cohort (Jiao *et al.* 2011, Scarpa *et al.* 2017). Additionally, the pro-apoptotic gene *CYFIP2* was mutated in four tumors. In two tumors, the exact same mutation was present, a so-called hotspot mutation. This validated mutation has never been reported before in pNEN and is predicted to be protein-damaging, warranting further studies into the role of *CYFIP2* in pNEN. Three mutations (one high-abundance and two low-abundance) were found in *SMAD4*. Unlike in small intestinal neuroendocrine neoplasms, where *SMAD4* loss is relatively common, the frequency of *SMAD4* mutations in pNEN has been the matter of debate (Bartsch *et al.* 1999, Perren *et al.* 2003, Banck *et al.* 2013). Multiple low-abundance recurrent mutations were identified, including a hotspot mutation in *PTCH2*. *PTCH2* encodes the Patched 2 protein, which is involved in hedgehog signaling (Smyth *et al.* 1999, Rahnama *et al.* 2004). *PTCH2* mutations have been found in basal cell carcinoma, medulloblastoma and rhabdomyosarcoma and myeloproliferative neoplasms (Smyth *et al.* 1999, Klein *et al.* 2016, Tæubner *et al.* 2018). However, this is the first time that hedgehog signaling has been implicated in pNENs. As the technical limitations of Sanger sequencing did not allow validation of this low-abundance mutation, further studies in replication cohorts are needed to confirm hedgehog signaling as a novel pathway in pNENs. Given that various hedgehog signaling inhibitors have been approved for use in basal cell carcinoma, confirmatory studies on the role of hedgehog signaling could open new therapeutic options for pNENs, harboring *PTCH2* mutations (Lacouture *et al.* 2016). Finally, the limited availability of fresh-frozen tissue in pNEN could hinder the implementation of next-generation sequencing technology in pNEN diagnostics. In contrast, archival tissue, necessary for histological diagnosis of pNEN, is frequently available and can be easily manipulated and stored in a cost-effective manner. A possible limitation of the use of FFPE is the induction of false-positive mutations by formalin fixation (Williams *et al.* 1999). These mutations often follow a deamination pattern, resulting in transitions (C>T or G>A). Hence, when formalin fixation would result in a considerable number of additional induced mutations, there would be an increase

in the number of transitions (C>T or G>A) in comparison to transversions (A>C or G>T). However, the ratio of transitions to transversion in this study is similar to transition-transversion ratios seen in normal human (germline) samples and in pNEN samples from fresh-frozen tissue (Jiao *et al.* 2011). Therefore, the impact of formalin fixation can be considered to be relatively limited. To further reduce any potential impact, the in-house developed pyAmpli tool filters specifically for mutations present in more than one amplicon and, thus, amplified DNA fragment (Beyens *et al.* 2017). As fixation-induced 'deamination' is stochastic and happens randomly in all DNA strands, the chance that two different DNA molecules have exactly the same formalin fixation induced is very limited. Hence, our study demonstrates that by using this approach archival FFPE tissue can be used reliably in genetic analysis of pNENs.

In conclusion, this study adds to the growing body of evidence on the broad genetic constitution of pNENs by demonstrating the presence of low-abundance mutations and genetic heterogeneity in pNENs. We highlight the importance of the *ATRX/DAXX* pathway by reporting the first-ever pNEN-specific protein-damaging hotspot mutation in *DAXX*, and uncover novel genes and pathways involved in pNENs, including pro-apoptotic *CYFIP2*, hedgehog signaling and the MAPK-ERK pathway.

Supplementary data

This is linked to the online version of the paper at <https://doi.org/10.1530/ERC-18-0120>.

Declaration of interest

Timon Vandamme: advisory role and speakers' fees for Ipsen and Novartis. Wouter de Herder: advisory role and speakers' fees for Ipsen and Novartis. Marc Peeters: advisory role and speakers' fees for Ipsen and Novartis. Matthias Beyens, Ken Op de Beeck, Fadime Dogan, Peter M van Koetsveld, Patrick Pauwels, Guy Van Camp, Leo J Hofland, Gitta Boons, Anne Schepers, Kimberley Kamp, Katharina Biermann: No conflicts of interest to declare.

Funding

This work was supported by the Flemish Agency of Scientific Research (FWO grant G.0327.13N) and the ENETS-Ipsen 2013 Translational Research Fellowship.

Author contribution statement

T V, M B, G B, A S performed the sequencing experiments. T V, M B, K O d B processed the experimental data, performed the analysis, drafted the manuscript and designed the figures. P P, K B and L J H performed pathological review of all tumor and normal samples and aided in patient selection. K K and W W D H aided in patient selection and collected clinicopathological data. L J H, W W D H, M P and G V C were involved in

planning and supervised the work. All authors discussed the results and commented on the manuscript.

Acknowledgements

The authors would like to thank Lesley De Backer from the Multidisciplinair Oncologisch Centrum Antwerpen and NETwerk for her support in collecting clinicopathological data of all patients included at the University Hospital Antwerp.

References

- Andrews S 2010 FastQC: a quality control tool for high throughput sequence data. Cambridge, UK: Babraham Institute. (available at: <http://www.bioinformatics.babraham.ac.uk/projects/fastqc>)
- Banck MS, Kanwar R, Kulkarni AA, Boora GK, Metge F, Kipp BR, Zhang L, Thorland EC, Minn KT, Tentu R, *et al.* 2013 The genomic landscape of small intestine neuroendocrine tumors. *Journal of Clinical Investigation* **123** 2502–2508. (<https://doi.org/10.1172/JCI67963>)
- Bartsch D, Hahn SA, Danichevski KD, Ramaswamy A, Bastian D, Galehdari H, Barth P, Schmiegel W, Simon B & Rothmund M 1999 Mutations of the DPC4/Smad4 gene in neuroendocrine pancreatic tumors. *Oncogene* **18** 2367–2371. (<https://doi.org/10.1038/sj.onc.1202585>)
- Beyens M, Boeckx N, Van Camp G, Op de Beeck K & Vandeweyer G 2017 pyAmpli: an amplicon-based variant filter pipeline for targeted resequencing data. *BMC Bioinformatics* **18** 554. (<https://doi.org/10.1186/s12859-017-1985-1>)
- Bosman FT, Carneiro F, Hruban RH & Theise ND 2010 *WHO Classification of Tumours of the Digestive System*. Lyon: IARC Press.
- Burrell RA, McGranahan N, Bartek J & Swanton C 2013 The causes and consequences of genetic heterogeneity in cancer evolution. *Nature* **501** 338–345. (<https://doi.org/10.1038/nature12625>)
- Carracedo A, Ma L, Teruya-Feldstein J, Rojo F, Salmena L, Alimonti A, Egia A, Sasaki AT, Thomas G, Kozma SC, *et al.* 2008 Inhibition of mTORC1 leads to MAPK pathway activation through a PI3K-dependent feedback loop in human cancer. *Journal of Clinical Investigation* **118** 3065–3074. (<https://doi.org/10.1172/JCI34739>)
- Cesare AJ & Reddel RR 2010 Alternative lengthening of telomeres: models, mechanisms and implications. *Nature Reviews Genetics* **11** 319–330. (<https://doi.org/10.1038/nrg2763>)
- Choi Y, Sims GE, Murphy S, Miller JR & Chan AP 2012 Predicting the functional effect of amino acid substitutions and indels. *PLoS ONE* **7** e46688. (<https://doi.org/10.1371/journal.pone.0046688>)
- Chou WC, Lin PH, Yeh YC, Shyr YM, Fang WL, Wang SE, Liu CY, Chang PM, Chen MH, Hung YP, *et al.* 2016 Genes involved in angiogenesis and mTOR pathways are frequently mutated in Asian patients with pancreatic neuroendocrine tumors. *International Journal of Biological Sciences* **12** 1523–1532. (<https://doi.org/10.7150/ijbs.16233>)
- Corbo V, Dalai I, Scardoni M, Barbi S, Beghelli S, Bersani S, Albarello L, Doglioni C, Schott C, Capelli P, *et al.* 2010 MEN1 in pancreatic endocrine tumors: analysis of gene and protein status in 169 sporadic neoplasms reveals alterations in the vast majority of cases. *Endocrine-Related Cancer* **17** 771–783. (<https://doi.org/10.1677/ERC-10-0028>)
- Crona J & Skogseid B 2016 GEP- NETS UPDATE: genetics of neuroendocrine tumors. *European Journal of Endocrinology* **174** R275–R290. (<https://doi.org/10.1530/EJE-15-0972>)
- Dasari A, Shen C, Halperin D, Zhao B, Zhou S, Xu Y, Shih T & Yao JC 2017 Trends in the incidence, prevalence, and survival outcomes in patients with neuroendocrine tumors in the United States. *JAMA Oncology* **3** 1335–1342. (<https://doi.org/10.1001/jamaoncol.2017.0589>)
- Elsasser SJ, Allis CD & Lewis PW 2011 Cancer. New epigenetic drivers of cancers. *Science* **331** 1145–1146. (<https://doi.org/10.1126/science.1203280>)
- Forbes SA, Beare D, Boutselakis H, Bamford S, Bindal N, Tate J, Cole CG, Ward S, Dawson E, Ponting L, *et al.* 2017 COSMIC: somatic cancer genetics at high-resolution. *Nucleic Acids Research* **45** D777–D783. (<https://doi.org/10.1093/nar/gkw1121>)
- Genomes Project C, Abecasis GR, Altshuler D, Auton A, Brooks LD, Durbin RM, Gibbs RA, Hurler ME & McVean GA 2010 A map of human genome variation from population-scale sequencing. *Nature* **467** 1061–1073. (<https://doi.org/10.1038/nature09534>)
- Gerstung M, Beisel C, Rechsteiner M, Wild P, Schraml P, Moch H & Beerenwinkel N 2012 Reliable detection of subclonal single-nucleotide variants in tumour cell populations. *Nature Communications* **3** 811. (<https://doi.org/10.1038/ncomms1814>)
- Grabner BC, Nardi V, Birsoy K, Possemato R, Shen K, Sinha S, Jordan A, Beck AH & Sabatini DM 2014 A diverse array of cancer-associated MTOR mutations are hyperactivating and can predict rapamycin sensitivity. *Cancer Discovery* **4** 554–563. (<https://doi.org/10.1158/2159-8290.CD-13-0929>)
- Greenman C, Stephens P, Smith R, Dalgliesh GL, Hunter C, Bignell G, Davies H, Teague J, Butler A, Stevens C, *et al.* 2007 Patterns of somatic mutation in human cancer genomes. *Nature* **446** 153–158. (<https://doi.org/10.1038/nature05610>)
- Heaphy CM, de Wilde RF, Jiao Y, Klein AP, Edil BH, Shi C, Bettgowda C, Rodriguez FJ, Eberhart CG, Hebbar S, *et al.* 2011 Altered telomeres in tumors with ATRX and DAXX mutations. *Science* **333** 425. (<https://doi.org/10.1126/science.1207313>)
- Jiao Y, Shi C, Edil BH, de Wilde RF, Klimstra DS, Maitra A, Schulick RD, Tang LH, Wolfgang CL, Choti MA, *et al.* 2011 DAXX/ATRX, MEN1, and mTOR pathway genes are frequently altered in pancreatic neuroendocrine tumors. *Science* **331** 1199–1203. (<https://doi.org/10.1126/science.1200609>)
- Jones S, Zhang X, Parsons DW, Lin JC, Leary RJ, Angenendt P, Mankoo P, Carter H, Kamiyama H, Jimeno A, *et al.* 2008 Core signaling pathways in human pancreatic cancers revealed by global genomic analyses. *Science* **321** 1801–1806. (<https://doi.org/10.1126/science.1164368>)
- Kim H, Lee JE, Cho EJ, Liu JO & Youn HD 2003 Menin, a tumor suppressor, represses JunD-mediated transcriptional activity by association with an mSin3A-histone deacetylase complex. *Cancer Research* **63** 6135–6139.
- Klein C, Zwick A, Kissel S, Forster CU, Pfeifer D, Follo M, Illert AL, Decker S, Benkler T, Pahl H, *et al.* 2016 Ptch2 loss drives myeloproliferation and myeloproliferative neoplasm progression. *Journal of Experimental Medicine* **213** 273–290. (<https://doi.org/10.1084/jem.20150556>)
- Koboldt DC, Zhang Q, Larson DE, Shen D, McLellan MD, Lin L, Miller CA, Mardis ER, Ding L & Wilson RK 2012 VarScan 2: somatic mutation and copy number alteration discovery in cancer by exome sequencing. *Genome Research* **22** 568–576. (<https://doi.org/10.1101/gr.129684.111>)
- Lacouture ME, Dreno B, Ascierto PA, Dummer R, Basset-Seguin N, Fife K, Ernst S, Licitra L, Neves RI, Peris K, *et al.* 2016 Characterization and management of hedgehog pathway inhibitor-related adverse events in patients with advanced basal cell carcinoma. *Oncologist* **21** 1218–1229. (<https://doi.org/10.1634/theoncologist.2016-0186>)
- Lek M, Karczewski KJ, Minikel EV, Samocha KE, Banks E, Fennell T, O'Donnell-Luria AH, Ware JS, Hill AJ, Cummings BB, *et al.* 2016 Analysis of protein-coding genetic variation in 60,706 humans. *Nature* **536** 285–291. (<https://doi.org/10.1038/nature19057>)
- Lewis PW, Elsaesser SJ, Noh KM, Stadler SC & Allis CD 2010 Daxx is an H3.3-specific histone chaperone and cooperates with ATRX in replication-independent chromatin assembly at telomeres. *PNAS* **107** 14075–14080. (<https://doi.org/10.1073/pnas.1008850107>)
- Li H & Durbin R 2009 Fast and accurate short read alignment with Burrows-Wheeler transform. *Bioinformatics* **25** 1754–1760. (<https://doi.org/10.1093/bioinformatics/btp324>)
- Li H, Handsaker B, Wysoker A, Fennell T, Ruan J, Homer N, Marth G, Abecasis G, Durbin R & Genome Project Data Processing S 2009 The sequence alignment/map format and SAMtools. *Bioinformatics* **25** 2078–2079. (<https://doi.org/10.1093/bioinformatics/btp352>)

- Lin SY & Elledge SJ 2003 Multiple tumor suppressor pathways negatively regulate telomerase. *Cell* **113** 881–889. ([https://doi.org/10.1016/S0092-8674\(03\)00430-6](https://doi.org/10.1016/S0092-8674(03)00430-6))
- Lynch M 2010 Rate, molecular spectrum, and consequences of human mutation. *PNAS* **107** 961–968. (<https://doi.org/10.1073/pnas.0912629107>)
- Mayakonda A & Koeffler P 2016 Maftools: efficient analysis, visualization and summarization of MAF files from large-scale cohort based cancer studies. *BioRxiv*. (<https://doi.org/doi.org/10.1101/052662>)
- Perren A, Saremaslani P, Schmid S, Bonvin C, Locher T, Roth J, Heitz PU & Komminoth P 2003 DPC4/Smad4: no mutations, rare allelic imbalances, and retained protein expression in pancreatic endocrine tumors. *Diagnostic Molecular Pathology* **12** 181–186. (<https://doi.org/10.1097/00019606-200312000-00001>)
- Pruitt KD, Brown GR, Hiatt SM, Thibaud-Nissen F, Astashyn A, Ermolaeva O, Farrell CM, Hart J, Landrum MJ, McGarvey KM, *et al.* 2014 RefSeq: an update on mammalian reference sequences. *Nucleic Acids Research* **42** D756–D763. (<https://doi.org/10.1093/nar/gkt1114>)
- Rahnama F, Toftgard R & Zaphiropoulos PG 2004 Distinct roles of PTCH2 splice variants in Hedgehog signalling. *Biochemical Journal* **378** 325–334. (<https://doi.org/10.1042/bj20031200>)
- Sadanandam A, Wullschlegel S, Lyssiotis CA, Grotzinger C, Barbi S, Bersani S, Korner J, Wafy I, Mafficini A, Lawlor RT, *et al.* 2015 A cross-species analysis in pancreatic neuroendocrine tumors reveals molecular subtypes with distinctive clinical, metastatic, developmental, and metabolic characteristics. *Cancer Discovery* **5** 1296–1313. (<https://doi.org/10.1158/2159-8290.CD-15-0068>)
- Scarpa A, Chang DK, Nones K, Corbo V, Patch AM, Bailey P, Lawlor RT, Johns AL, Miller DK, Mafficini A, *et al.* 2017 Whole-genome landscape of pancreatic neuroendocrine tumours. *Nature* **543** 65–71. (<https://doi.org/10.1038/nature21063>)
- Schwarz JM, Cooper DN, Schuelke M & Seelow D 2014 MutationTaster2: mutation prediction for the deep-sequencing age. *Nature Methods* **11** 361–362. (<https://doi.org/10.1038/nmeth.2890>)
- Sherry ST, Ward MH, Kholodov M, Baker J, Phan L, Smigielski EM & Sirotkin K 2001 dbSNP: the NCBI database of genetic variation. *Nucleic Acids Research* **29** 308–311. (<https://doi.org/10.1093/nar/29.1.308>)
- Shi C, Gonzalez RS, Zhao Z, Koyama T, Cornish TC, Hande KR, Walker R, Sandler M, Berlin J & Liu EH 2015 Liver metastases of small intestine neuroendocrine tumors: Ki-67 heterogeneity and World Health Organization grade discordance with primary tumors. *American Journal of Clinical Pathology* **143** 398–404. (<https://doi.org/10.1309/AJCPQ55SKOCYFZHN>)
- Singhi AD, Liu TC, Roncaioli JL, Cao D, Zeh HJ, Zureikat AH, Tsung A, Marsh JW, Lee KK, Hogg ME, *et al.* 2017 Alternative lengthening of telomeres and loss of DAXX/ATRX expression predicts metastatic disease and poor survival in patients with pancreatic neuroendocrine tumors. *Clinical Cancer Research* **23** 600–609. (<https://doi.org/10.1158/1078-0432.CCR-16-1113>)
- Smyth I, Narang MA, Evans T, Heimann C, Nakamura Y, Chenevix-Trench G, Pietsch T, Wicking C & Wainwright BJ 1999 Isolation and characterization of human patched 2 (PTCH2), a putative tumour suppressor gene in basal cell carcinoma and medulloblastoma on chromosome 1p32. *Human Molecular Genetics* **8** 291–297. (<https://doi.org/10.1093/hmg/8.2.291>)
- Stratton MR, Campbell PJ & Futreal PA 2009 The cancer genome. *Nature* **458** 719–724. (<https://doi.org/10.1038/nature07943>)
- Taebner J, Brozou T, Qin N, Bartl J, Ginzl S, Schaper J, Felsberg J, Fulda S, Vokuhl C, Borkhardt A, *et al.* 2018 Congenital embryonal rhabdomyosarcoma caused by heterozygous concomitant PTCH1 and PTCH2 germline mutations. *European Journal of Human Genetics* **26** 137–142. (<https://doi.org/10.1038/s41431-017-0048-4>)
- Thorvaldsdottir H, Robinson JT & Mesirov JP 2012 Integrative genomics viewer (IGV): high-performance genomics data visualization and exploration. *Briefings in Bioinformatics* **14** 178–192. (<https://doi.org/10.1093/bib/bbs017>)
- Tsiatis AC, Norris-Kirby A, Rich RG, Hafez MJ, Gocke CD, Eshleman JR & Murphy KM 2010 Comparison of Sanger sequencing, pyrosequencing, and melting curve analysis for the detection of KRAS mutations: diagnostic and clinical implications. *Journal of Molecular Diagnostics* **12** 425–432. (<https://doi.org/10.2353/jmoldx.2010.090188>)
- Valentino JD, Li J, Zaytseva YY, Mustain WC, Elliott VA, Kim JT, Harris JW, Campbell K, Weiss HL, Wang C, *et al.* 2014 Co-targeting the PI3K and RAS pathways for the treatment of neuroendocrine tumors. *Clinical Cancer Research* **20** 1212–1222. (<https://doi.org/10.1158/1078-0432.CCR-13-1897>)
- Vandeweyer G, Van Laer L, Loeys B, Van den Bulcke T & Kooy RF 2014 VariantDB: a flexible annotation and filtering portal for next generation sequencing data. *Genome Medicine* **6** 74. (<https://doi.org/10.1186/s13073-014-0074-6>)
- Vandamme T, Beyens M, Peeters M, Van Camp G & Op de Beek K 2015a Next generation exome sequencing of pancreatic neuroendocrine tumor cell lines BON-1 and QGP-1 reveals different lineages. *Cancer Genetics* **208** 523–523. (<https://doi.org/10.1016/j.cancergen.2015.07.003>)
- Vandamme T, Peeters M, Dogan F, Pauwels P, Van Assche E, Beyens M, Mortier G, Vandeweyer G, de Herder W, Van Camp G, *et al.* 2015b Whole-exome characterization of pancreatic neuroendocrine tumor cell lines BON-1 and QGP-1. *Journal of Molecular Endocrinology* **54** 137–147. (<https://doi.org/10.1530/JME-14-0304>)
- Vandamme T, Beyens M, de Beek KO, Dogan F, van Koetsveld PM, Pauwels P, Mortier G, Vangestel C, de Herder W, Van Camp G, *et al.* 2016 Long-term acquired everolimus resistance in pancreatic neuroendocrine tumours can be overcome with novel PI3K-AKT-mTOR inhibitors. *British Journal of Cancer* **114** 650–658. (<https://doi.org/10.1038/bjc.2016.25>)
- Wagle N, Grabiner BC, Van Allen EM, Amin-Mansour A, Taylor-Weiner A, Rosenberg M, Gray N, Barletta JA, Guo Y, Swanson SJ, *et al.* 2014 Response and acquired resistance to everolimus in anaplastic thyroid cancer. *New England Journal of Medicine* **371** 1426–1433. (<https://doi.org/10.1056/NEJMoa1403352>)
- Wang K, Li M & Hakonarson H 2010 ANNOVAR: functional annotation of genetic variants from high-throughput sequencing data. *Nucleic Acids Research* **38** e164. (<https://doi.org/10.1093/nar/gkq603>)
- Williams C, Ponten F, Moberg C, Soderkvist P, Uhlen M, Ponten J, Sitbon G & Lundeberg J 1999 A high frequency of sequence alterations is due to formalin fixation of archival specimens. *American Journal of Pathology* **155** 1467–1471. ([https://doi.org/10.1016/S0002-9440\(10\)65461-2](https://doi.org/10.1016/S0002-9440(10)65461-2))
- Yao JC, Shah MH, Ito T, Bohas CL, Wolin EM, Van Cutsem E, Hobday TJ, Okusaka T, Capdevila J, de Vries EG, *et al.* 2011 Everolimus for advanced pancreatic neuroendocrine tumors. *New England Journal of Medicine* **364** 514–523. (<https://doi.org/10.1056/NEJMoa1009290>)
- Zitzmann K, Ruden J, Brand S, Goke B, Lichtl J, Spottl G & Auernhammer CJ 2010 Compensatory activation of Akt in response to mTOR and Raf inhibitors – a rationale for dual-targeted therapy approaches in neuroendocrine tumor disease. *Cancer Letters* **295** 100–109. (<https://doi.org/10.1016/j.canlet.2010.02.018>)

Received in final form 16 July 2018

Accepted 18 July 2018

Accepted Preprint published online 18 July 2018